MENTATION PAGE

Form Approved
OMB No 0704-0188

REPORT DATE	3. REPORT TYPE AND DATES COVERED
February 1993	Annual Jan. 1, 1992 - Dec. 31, 1992

4. TITLE AND SUBTITLE

Diamond homoepitaxy by chemical vapor deposition

5. FUNDING NUMBERS

N00014-92-J-1421

6. AUTHOR(S)

Andrzej Badzian and Teresa Badzian

7. PERFORMING ORGANIZATION NAME(S) AND ADDRESS(ES)

The Pennsylvania State University
Materials Research Laboratory
University Park, PA 16802

8. PERFORMING ORGANIZATION REPORT NUMBER

9. SPONSORING / MONITORING AGENCY NAME(S) AND ADDRESS(ES)

Department of the Navy
Office of the Chief of Naval Research
800 North Quincy Street, Code ONR-1114
Arlington, VA 22217

10. SPONSORING / MONITORING AGENCY REPORT NUMBER

130 8

11. SUPPLEMENTARY NOTES

12a. DISTRIBUTION / AVAILABILITY STATEMENT

Distribution Unlimited
Approved for Public Release

12b. DISTRIBUTION CODE

13. ABSTRACT *(Maximum 200 words)*

Gem-quality single crystals of diamond were grown by homoepitaxy using microwave plasma assisted chemical vapor deposition. Raman spectra of the (001) films show very low background and the narrowest width at half maximum of the 1332 cm^{-1} peak was 1.7 cm^{-1}. A prism crystal 1.2 mm high was grown in the <110> direction at 1200°C and 1% CH_4 in H_2. Its Raman peak has a width of 2.7 cm^{-1}.

Homoepitaxy is a tool used to study growth processes by analyzing the geometrical details of surfaces morphologies. Growth steps on the (001) surface develop in the <110> directions while triangular plates appear on the (111) surface. The (110) atomic plane does not appear in the <110> growth direction with microfaceted (111) and (111) planes present instead.

Crystal structure of diamond grown in the (001), (111), (110) substrates, as well as growth sectors developed in conjunction with this epitaxy, were studied by X-ray diffraction techniques: Laue, oscillation and rotation methods. Atomic force microscopy reached atomic resolution on the (001) surface.

The presence of a 2.12 Å reflection demonstrated distortion of cubic symmetry and deformation of carbon tetrahedra in the case of (111) epitaxy. In the (110) growth sector a polytype/superstructure network with periodicity three times larger than that of the cubic form was determined. In general it is possible to form tetrahedral carbons with the sequence of tetrahedra different from that of cubic and hexagonal diamonds.

14. SUBJECT TERMS	15. NUMBER OF PAGES
Diamond, Chemical Vapor Deposition, Homoepitaxy, Stacking Faults	11
	16. PRICE CODE

17. SECURITY CLASSIFICATION OF REPORT	18. SECURITY CLASSIFICATION OF THIS PAGE	19. SECURITY CLASSIFICATION OF ABSTRACT	20. LIMITATION OF ABSTRACT
Unclassified	Unclassified	Unclassified	UL

NSN 7540-01-280-5500

Standard Form 298 (Rev. 2-89)
Prescribed by ANSI Std. 239-18
298-102

Diamond and Related Materials, 00 (1993) 00–00

Diamond homoepitaxy by chemical vapor deposition

Andrzej Badzian and Teresa Badzian
Materials Research Laboratory, The Pennsylvania State University, University Park, PA 16802 (USA)

Abstract

Gem-quality single crystals of diamond were grown by homoepitaxy using microwave plasma assisted chemical vapor deposition. Raman spectra of the (001) films show very low background and the narrowest width at half maximum of the 1332 cm^{-1} peak was 1.7 cm^{-1}. A prism crystal 1.2 mm high was grown in the ⟨110⟩ direction at 1200 °C and 1% CH_4 in H_2. Its Raman peak has a width of 2.7 cm^{-1}.

Homoepitaxy is a tool used to study growth processes by analyzing the geometrical details of surfaces morphologies. Growth steps on the (001) surface develop in the ⟨110⟩ directions while triangular plates appear on the (111) surface. The (110) atomic plane does not appear in the ⟨110⟩ growth direction with microfaceted (111) and ($11\bar{1}$) planes present instead.

Crystal structure of diamond grown on the (001), (111), (110) substrates, as well as growth sectors developed in conjunction with this epitaxy, were studied by X-ray diffraction techniques: Laue, oscillation and rotation methods. Atomic force microscopy reached atomic resolution on the (001) surface.

The presence of a 2.12 Å reflection demonstrates distortion of cubic symmetry and deformation of carbon tetrahedra in the case of (111) epitaxy. In the ⟨110⟩ growth sector a polytype/superstructure network with periodicity three times larger than that of the cubic form was determined. In general it is possible to form tetrahedral carbons with the sequence of tetrahedra different from that of cubic and hexagonal diamonds.

1. CVD diamond gem crystals

In 1797 chemists discovered that diamond crystals were almost pure carbon [1]. Why not prepare them in a laboratory? This was the beginning of a long history of efforts to duplicate the processes of nature. This duplication never occurred; instead, new laboratory processes were developed. The high pressure/high temperature (HP/HT) process developed at the GE laboratory and followed by the Sumitomo Electric and De Beers Companies demonstrated the feasibility of growing single crystals of diamond up to 12 mm long. High quality gem-type crystals of isotopically pure ^{12}C, of ^{13}C and of their solid solutions were successfully synthesized at GE and the enhancement of the thermal conductivity (pure ^{12}C) was demonstrated [2, 3].

CVD methods are behind HP/HT techniques in the crystal size competition. The first single crystals of diamond, up to 100 μm, were grown by microwave plasma CVD on silicon substrate [4], and homoepitaxial growth of 60 μm and thicker CVD film [5] demonstrated the feasibility of preparing gem-quality crystals. IR spectra of CVD homoepitaxial films (up to 250 μm thick) are similar to type IIa natural diamond with respect to one-phonon, two-phonon and C–H stretching bond vibration, but differ in the level of scattering [5]. High growth rates and high quality films were achieved using the flame method in the ⟨110⟩ direction at 900 °C [6, 7] and for (100) epitaxy at 1200–1500 °C [8, 9].

The ultimate goal of homoepitaxy is to demonstrate the potential of CVD methods to grow single crystals of diamond comparable in size and crystallographic quality with natural and HP/HT crystals.

2. Goals of homoepitaxy

Early experiments began with the concept of diamond homoepitaxy. Research focused on how to initiate and continue the building of a diamond lattice while avoiding graphite conucleation. Heterogeneous decomposition reactions of CH_4 and CO became fruitful approaches and were transformed into a practical diamond crystallization process from the gas phase. This process is possible because of selective surface forces which allow the building of a diamond lattice to continue. Eversole [10] and Angus *et al.* [11] used diamond powders in their experiments to increase the surface deposition area. Spitsyn used natural diamond crystals in his early experiments with CBr_4 and CJ_4 and was successful in the chemical transport reaction [12, 13]. Microwave plasma CVD has been applied in the case of the (100), (111) and (110) homoepitaxy [14–16] and the tungsten filament method was explored further [17, 18].

Scientific and engineering goals of homoepitaxy are manifold.

(a) Homoepitaxy is used to study the growth process because one can separate growth sectors. Thin CVD

0925-9635/93/$6.00

films can be grown on the desired surfaces that are cut along the crystallographic planes or inclined to them. Thick CVD films or crystals can be grown on the top and on the side surfaces of a parallelepiped cut along desired planes of diamond crystal substrate. Natural, and as-grown HP/HT crystals (like cubooctahedra), are also appropriate for homoepitaxy. In the last cases, several growth sectors appear simultaneously.

(b) Surface morphology, which reveals the state of the surface at a given growth moment, can be studied by a variety of microscopic techniques.

(c) Growth defects identified in a given growth sector can be a source of information regarding the growth process.

(d) Process parameters can be related to the particular growth direction providing a guide for growth process modeling.

(e) Large epitaxial surfaces facilitate the measurement of physical properties. This is an important factor in the case of diamond because of the anisotropy of the properties related to crystal structure.

(f) Homoepitaxial growth enables one to study the tetrahedral form of carbon which has an atomic structure distinctly different from that of cubic diamond.

The aim of this paper is to present the results of a study of diamond homepitaxy conducted with the help of microwave plasma CVD. The research focused on: (1) the chemical purity of the films; (2) the crystal structure—defects—deviation from cubic symmetry; and (3) the surface morphology and geometry of the crystallization front.

3. CVD diamonds as new materials

The name "diamond" is given to a crystal of carbon which possesses a cubic, tetrahedral structure. This is the case of natural and HP/HT crystals because the growth processes favor the cubic structure. CVD growth techniques allow the crystallization of the cubic form but, in contrast to the natural process and the HP/HT process, opens the door to a realm of polytypes/superstructures. Polytypes are related to an alternating stacking sequence in one dimension. In the case of diamond, this is the ⟨111⟩ direction. CVD processes also enhance the frequency of twinning. The known forms of tetrahedral carbons are cubic diamond and hexagonal diamond (lonsdaleite).

Modification of diamond structure, which takes place during the CVD process conducted in the binary C–H gas system, is a consequence of surface reactions which proceed differently on different crystallographic surfaces and for different process parameters. This growth proceeds under the flux of atomic hydrogen. Structure modification may also take place for ternary gas systems, like C–H–B, C–H–N, C–H–O, C–H–Si, in a variety of ways.

In Table 1, several crystal forms are listed which, in our opinion, are distinct enough to be treated separately. The distinction of the crystal forms in Table 1 is based on particular structural or spectral features that are reproducible for a given process. On this basis, we think that we are dealing with different CVD "diamond" materials.

4. Chemical compositions of CVD diamonds

CVD diamonds grown by microwave plasma CVD in a C–H environment are contaminated by hydrogen. The lowest level of hydrogen known to the authors is 350 ppm for polycrystalline films and about 1000 ppm for the (001) epitaxial film. These results were obtained by nuclear reaction with ^{15}N analyses. Contamination by other elements depends on precautions made to avoid air leaks, etching reactor walls or substrate holder. The lowest limits for elements like N, O or Si can be below ppm level. Typical spectra obtained by secondary ion mass spectrometry, X-ray photoelectron spectroscopy and Auger Electron spectroscopy, performed in a routine manner, do not reveal impurities. This indicates that CVD material has much lower impurity levels than the natural crystals.

5. Crystal structure of CVD materials

It is highly desirable to demonstrate the ability of the CVD method to prepare large-area single-crystal diamond films. Limited progress with heteroepitaxy [19] keeps interest in homoepitaxial growth high. Homoepitaxial growth studies focus on the conditions at which secondary nucleation is limited. Secondary nucleation starts mostly with crystal lattice twinning. In the ⟨111⟩ growth sector, a high density of stacking faults was revealed by transmission electron microscopy (TEM) [20, 21]. Graphite inclusions oriented with respect to the diamond matrix were also detected [22]. Graphite inclusions disappear, however, when H° flux directed toward the growing diamond surface is sufficiently intense.

In addition to the cubic form of diamond, we are dealing with disordered forms of carbon as shown in Table 1.

Diamond belongs to the group of tetrahedral structures. A tetrahedron can be considered as a subunit in such networks. The basic tetrahedral structures like ZnS and SiC are cubic (sphalerite), hexagonal (wurtzite) and have polytypes [23]. The polytypes have two dimensions of the unit cell in common, when the third dimension varies. Before successful synthesis in the laboratory it

TABLE 1. Tentative list of tetrahedral forms of carbon

1	Cubic diamond of high crystallographic perfection	(001) epitaxy 850–900 °C,	Raman peak FWHM 1.7 cm^{-1}
		1% CH_4 (001) epitaxy 1200 °C	FWHM 2.0 cm^{-1}
		⟨110⟩ growth 1200 °C	FWHM 2.6 cm^{-1}
2	Triple periodicity "polytype"	900 °C, 1% CH_4 single crystal growth sector ⟨110⟩	Is yellow luminescence related to N?
3	Twin composite	950 °C, 1% CH4 ⟨111⟩ epitaxy twin domains organized in ⟨112⟩	X-ray; non-cubic 2.12 Å reflection no Raman peak 1445 cm^{-1} luminescence
4	Hexagonal diamond stacking	N influence (a) $CH_4 + N_2$ synthesis	X-ray band 2.19 Å 220 reflection shifted to higher θ, band in Raman 1540 cm^{-1}
		(b) addition of N_2 to CH_4/H_2 plasma	
5	Disordered diamond	Si influence Vacancy formation Si incorporation 1.5% at 900–1200 °C	X-ray peaks decrease Raman peak decrease GRI increase New Raman 1540 cm^{-1}
6	Solid solution of boron	B enhances cubic stacking B is dissolved in the diamond lattice	Raman peak wider, background decrease
7	Diamonds from CH_3 OH and alcohols	O influence enhanced stacking disorder	Strong Raman band at 1540 cm^{-1}

was suggested in 1951 by Vand that diamond might exhibit polytypism [24]. Later, hexagonal diamond structure was predicted [25] and synthesized under high pressure [26]. Tetrahedral representation of diamond structures is shown in Fig. 1 [27]. Hexagonal and cubic diamond differ only in the stacking of tetrahedra. When the stacking sequence is altered we are dealing with stacking fault. When the tetrahedra are reversed according to the mirror plane, we are dealing with a (111) twin.

There are many approaches to explain the phenomenon of polytypism. The approach proposed by Weltner introduced the concept of "internal rotation" forces which suggest distortion of the regular tetrahedron in polytypes [28]. Polytypes have a multitude of possible internal rotations around a three-fold axis; two are illustrated in Figs. 1(a) and 1(b).

Diamond polytypes were observed for particles about 0.1 μm in size by electron diffraction [29, 30]. In this

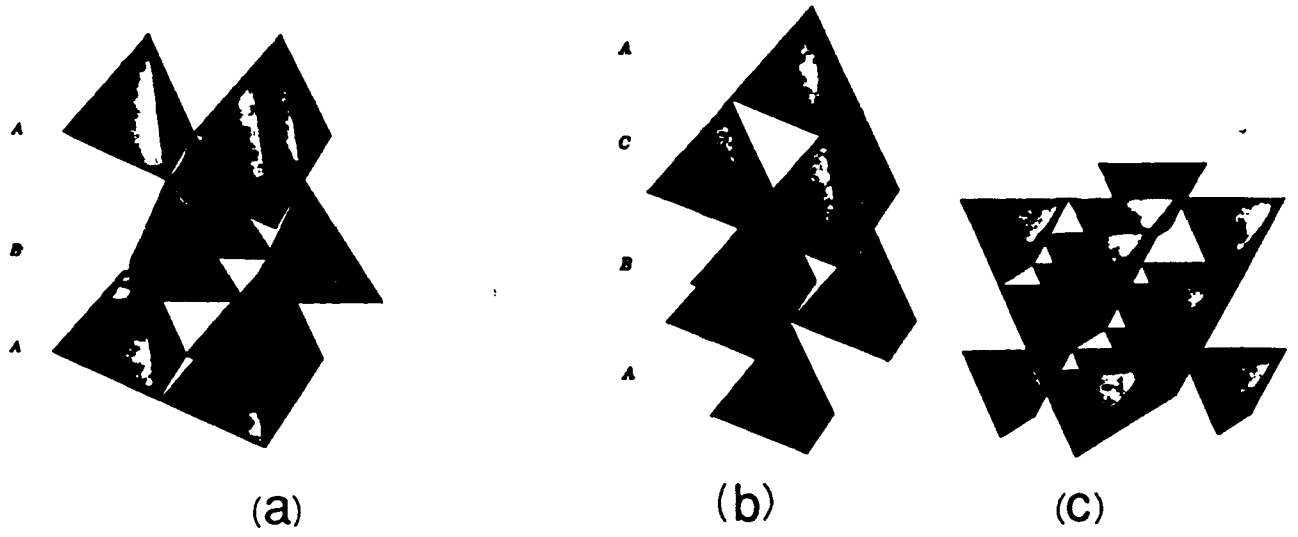

Fig. 1. Tetrahedral representation of (a) hexagonal (b) cubic (⟨111⟩ vertical) diamond structures (c) cubic diamond with ⟨001⟩ vertical, the ⟨110⟩ tilted to the plane of the figure. After Belov [27].

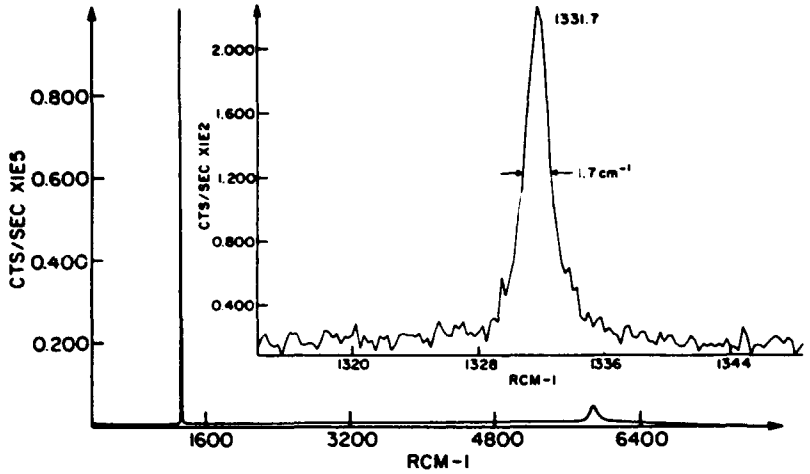

Fig. 2. Raman spectrum of diamond film grown on the (001) surface of type Ia natural diamond crystal at 900 °C, 80 Torr and 1% CH_4 in H_2.

paper, we report X-ray diffraction data for homoepitaxial films which indicate distortion of the cubic diamond structure.

6. Growth in the ⟨001⟩ direction

In the case of binary gas system C–H, our experiments indicate that growth in the ⟨001⟩ direction produces single-crystal diamond films of relatively high crystallographic perfection. At 1% CH_4 in H_2 and in a 850–900 °C temperature range, diamond films (up to 250 μm thick) were grown on the (001) natural and HP/HT diamond substrates. Raman spectra shows only the 1332 cm^{-1} peak and very low background. The narrowest diamond peak was measured for 18 μm thick film. The full width at half maximum (FWHM) is 1.7 cm^{-1}, which corresponds to the narrowest natural diamond Raman peak (Fig. 2). Most frequently, the FWHM is in the range 2.0–2.5 cm^{-1}. The contribution of the grown layer and the substrate was distinguished by measurements of the FWHM of the substrate before deposition. Type Ia natural diamond crystals used in our experiments showed FWHM in the range 2.2–2.7 cm^{-1}

A diamond film 60 μm thick on type IIa natural diamond substrate has been evaluated more extensively. A microscopic image under cross polaroids revealed stresses and stratification [31]. Cathodoluminescence spectra of a cross-sectional sample were also presented at the same conference [32]. With X-ray diffraction, we investigated the crystallographic relationship between CVD film and the substrate. Using Laue and rotation crystal methods, we came to the conclusion that both the substrate and CVD film form one single crystal. No misorientation was detected. There was no appreciable X-ray diffuse scattering coming from the CVD film.

It is worth mentioning that the substrate IIa type crystal plate with (001) top surface had the side surfaces cut approximately along {230} planes. We think that this particular configuration of crystallographic planes enabled the growth of single crystals around the substrate plate. Oblique faces were formed at the edges and vertices. For example, at the top surface an inclined plane was developed which correspond to (2. 3. 12). The face was 6.5° off the (001) and was 80 μm wide. Such vicinal surfaces were discussed for silicon in the framework of stabilities of single-layer and bi-layer steps [33]. atomic force microscope

Growth on the (001) surface proceeds as a step growth along the ⟨110⟩ crystallization fronts (Fig. 3). The fronts are not regular as shown in Fig. 3. The ⟨110⟩ steps are also seen with (AFM) Fig. 4(g). The scans were done on a 0.3 μm thick film along the ⟨110⟩ direction. On the

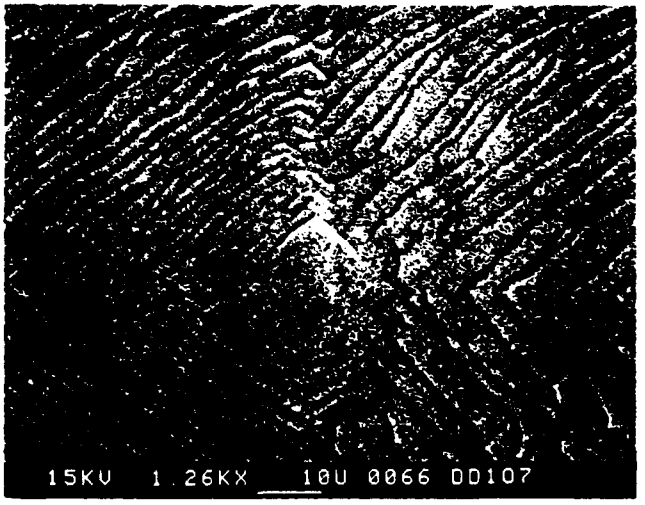

Fig. 3. Morphology of the (001) surface of homoepitaxial film grown in conditions specified in Fig. 2.

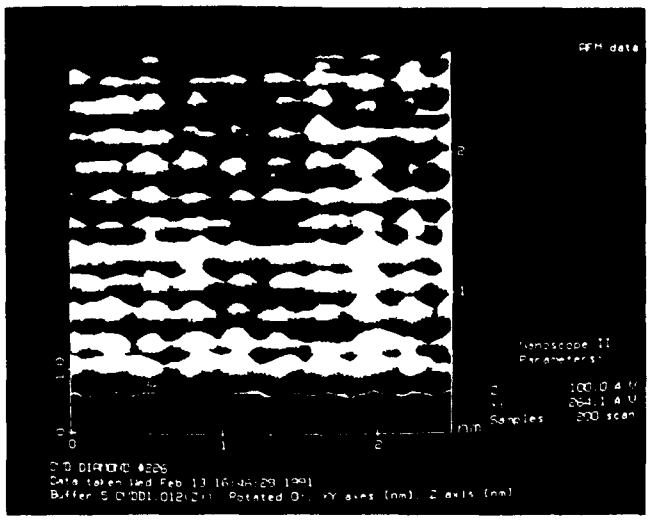

(a)

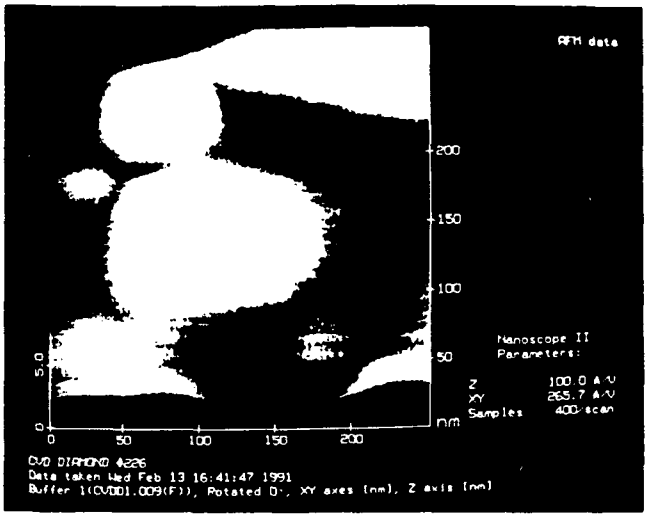

(c)

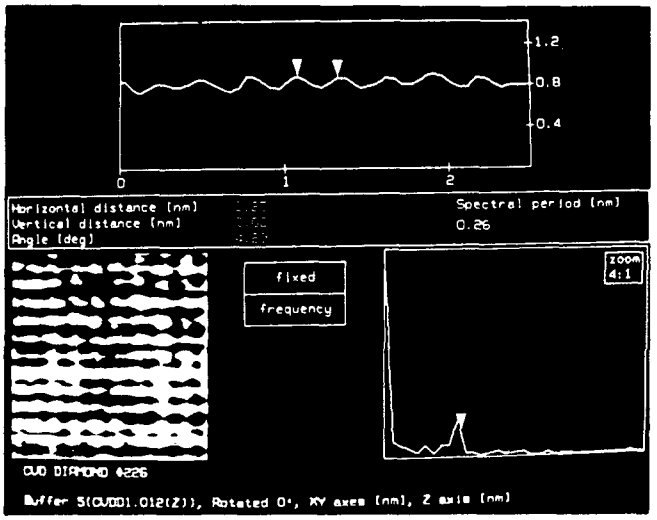

(b)

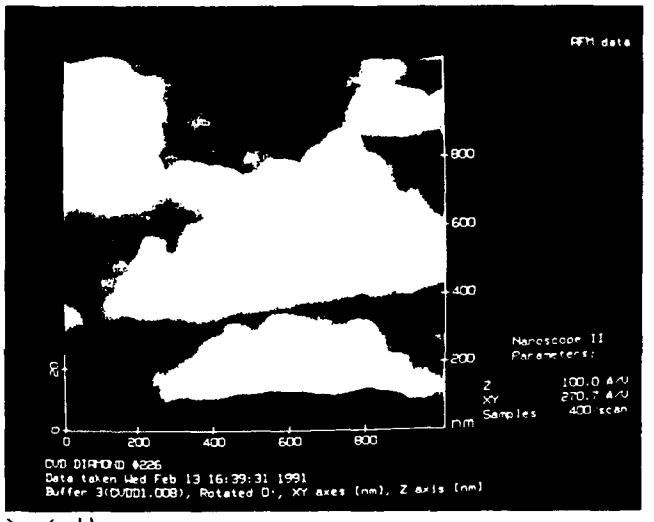

(d)

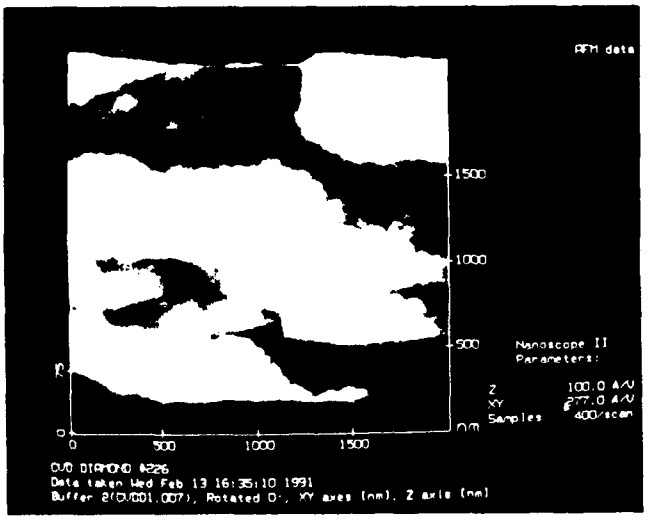

(e)

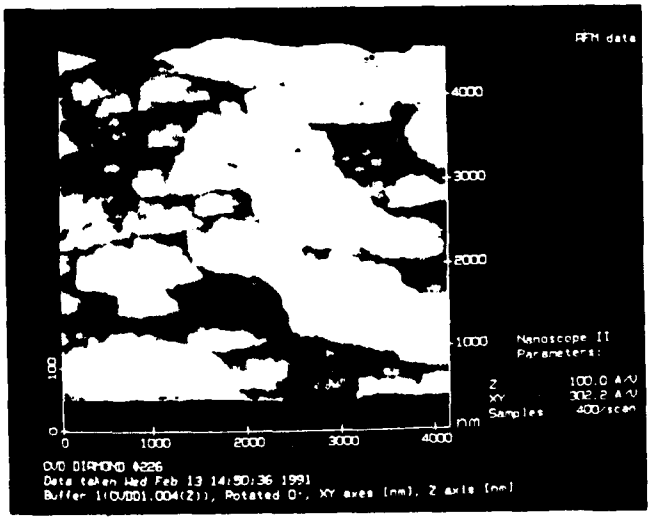

(f)

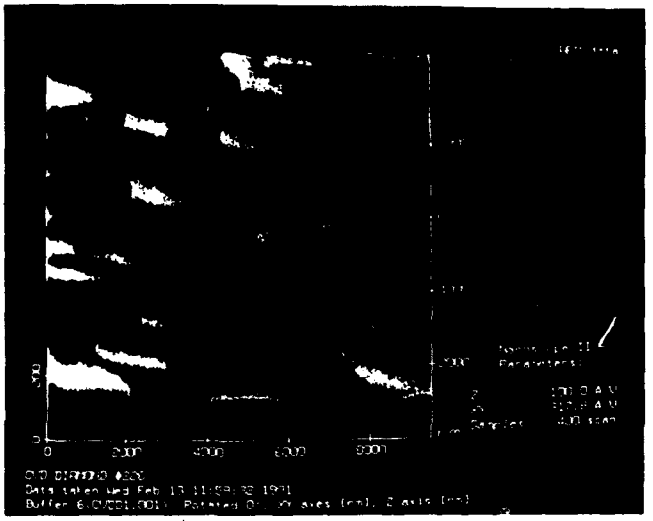

(g)

Fig. 4. Atomic force microscope images of the (001) surface of homoepitaxial film 0.3 μm thick grown on type IIa substrate at 0.8% CH4 and 900 °C. The AFM images were taken by Mark Anderson at the Jet Propulsion Laboratory, Pasadena, CA. (a) An image of a flat area. Scale is in nanometers. (b) Fourier transform of the image shown in (a) indicating periodicity about 2.5 Å. The arrow on the graph indicates 0.26 nm. Corrugation of the surface is shown in the top graph. The repetition distance is indicated by arrows. (c), (d), (e), (f), (g) images were taken at decreasing magnification. Irregular growth steps are seen on these images.

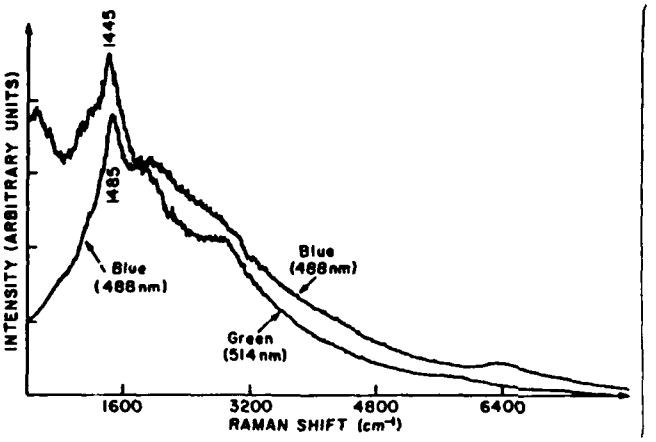

Fig. 5. Spectra taken with Raman spectrometer (for two excitation energies) on the top of 100 μm thick film grown on the face of type Ia crystal at 950 °C and 1% CH_4.

flat part of diamond (001) surfaces, the features are arranged periodically with 2.5 Å distance as was given by the Fourier transform. This corresponds to the atomic spacing in the ⟨110⟩ direction. It means that atomic resolution was achieved. It looks like regularly arranged rows and the corrugation on the ripples is about 1.6 Å (Fig. 4).

The regular array of features on AFM image does not correspond to STM images which show dimers [34]. These two microscopic methods are based on different physical principles, so we can expect different images; also hydrogenation of the diamond surface can be reflected differently. Hydrogenation itself can lead to monomer (1 × 1)H phase or to (2 × 1)H phase. To compare the situations it is necessary to have similar surface treatment in the last moment of the process.

Homoepitaxy on the (001) surface at 900 °C is disturbed by the formation of hillocks. The hillocks on thicker films (approximately 100 μm) form craters. Spectrum taken of such a crater with a micro-Raman spectrometer showed features described in the section about the (111) epitaxy, but no 1332 cm^{-1} peak was found (Fig. 5).

When growth was conducted at 1200 °C the hillocks have regular form. A micro-Raman spectrum taken on the top of the growth figure does not differ from that taken on a flat area of the homoepitaxial film. This spectrum shows a low level of luminescence and the FWHM of 1332 cm^{-1} peak was 2.1 cm^{-1}. In summary, growth at temperatures higher than 1100 °C is beneficial for film quality.

7. Growth in the ⟨111⟩ direction

When growth starts on the (111) surface, epitaxy is usually lost after a few micrometers and film become polycrystalline. Growth in the ⟨111⟩ direction is sensitive to defect propagation. This propagation also appears during the growth of other tetrahedral structures. Growth (from gallium solution) of GaP_xAs_{1-x}, $0 < x < 1$ mixed crystals develops a displacement disorder of P and As atoms on the P,As terminated side of plate-like crystals. The displacement disorder of atoms was not observed on the gallium side. [illegible] We used it was in the ⟨$\bar{1}\bar{1}\bar{1}$⟩ growth direction. The disorder will appear as an increase of the lattice constant measured along the ⟨111⟩ direction as the crystal grows. When the crystal was annealed after the growth process, the displacement disorder disappeared and the gradient of the lattice constant vanished. The displacement disorder was observed as the shift and the broadening of the *hhh* reflections as compared with sharp $\bar{h}\bar{h}\bar{h}$ [35].

Defects propagation means an increase of defect density as growth proceeds. Probably this effect makes it difficult to control diamond epitaxy on the (111).

In the case of diamond, micro-twinning on the {111} planes developed crystal domains oriented in the ⟨112⟩ direction. The domains themselves are distorted by stacking faults. A combination of these defects contributes to the disappearance of the Raman peak at 1332 cm^{-1} and the appearance of other types of scattering (Fig. 5). The maximum at 1445 cm^{-1} taken with the green line (514.5 nm) does not appear to be

Raman scattering because it shifts to 1485 cm^{-1} with the blue line (488 nm). The shift also does not follow a luminescence rule. This rule, widely accepted, requires the luminescence spectra be measured with two different excitation lines and photon energy assigned to the spectral features should be the same. The corresponding energies for the maxima shown in Fig. 5 are different: 2.23 eV and 2.35 eV. This type of spectrum is reproducible. We have no explanation for the shift of the maximum.

In some cases it was possible to avoid random, polycrystalline growth. Below we describe the case of oriented growth. Figure 6 shows the top surface of 100 μm thick, transparent film. The experiments were conducted at 950 °C and CH_4 concentration in H_2 below 1% CH_4. The choice of 950 °C for growth was made in conjunction to surface reconstruction [36] and the reverse of orientation of etch pits [37] which take place at this temperature.

An X-ray Laue photograph taken in the ⟨111⟩ direction indicates oriented domains. In Fig. 7 three X-ray elongated reflections correspond to the angular distribution of microdomains. Further, we found that 111 reflection (2.06 Å) has a satellite reflection 2.12 Å [5]. The 2.06 Å and 2.12 Å reflections appear as a doublet in the rocking curve. X-ray photographic measurements were performed with a standard. Diamond crystal powder was glued to the 111 surface. Confirmation of the 2.12 Å value was obtained from X-ray diffractometer measurements. The peak height ratio of the 2.12 Å reflection to the 2.06 Å reflection was 0.68. The satelite peak is as sharp as that of 2.06 Å. The 2.12 Å reflection is sharp and was reproduced in samples obtained in different growth conditions. This reflection

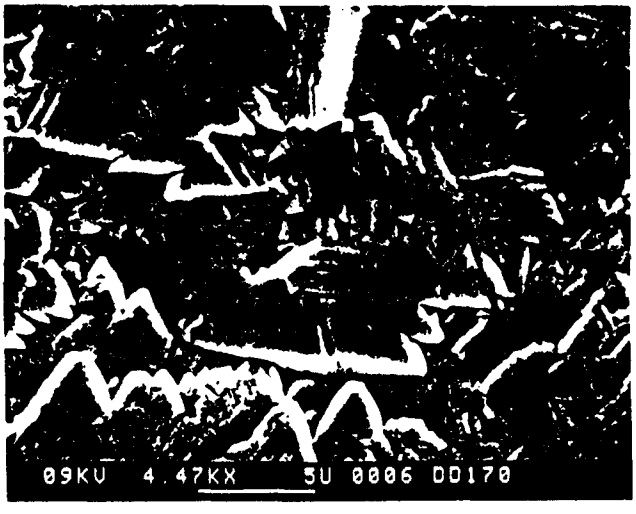

Fig 6. Morphology of the film described in Fig. 5. SEM secondary electron image.

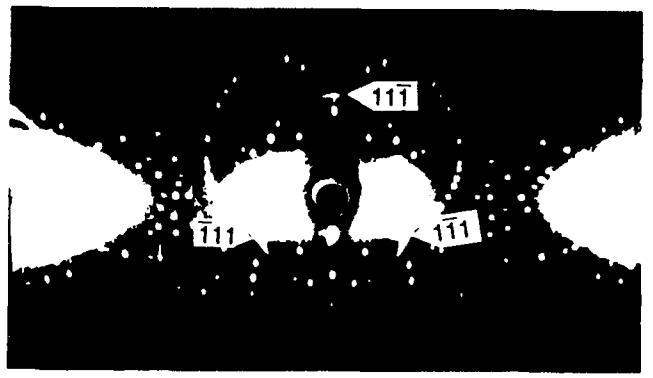

Fig. 7. Laue photograph taken along the ⟨111⟩ direction in the cylindrical camera (57.3 mm diameter). Three elongated reflections which are related to the 111, 1$\bar{1}$1 and 11$\bar{1}$ reciprocal lattice points, indicate oriented growth. Cu radiation.

is different from the (100) of hexagonal diamond where d is 2.18 Å.

If we assume that this reflection corresponds to a new interplanar distance it will mean that the diamond lattice is distorted.

In the perfect diamond lattice $d_{111} = 2.06$ Å corresponds to the height of a regular tetrahedron. The appearance of a 2.12 Å reflection can be interpretated as a new plane parallel to diamond (111).

This can indicate that some tetrahedra are elongated in the ⟨111⟩ direction as was observed for SiC [28]. We have observed the shrinking of the diamond lattice in the ⟨110⟩ direction.

In summary epitaxial growth in the ⟨111⟩ direction at 950 °C results in a non-cubic form of tetrahedral carbon [38]. More study on crystal structure is required to determine stacking and deformation of the tetrahedra.

8. Growth in the ⟨110⟩ direction

Epitaxy on the (110) surface, as in the case of the ⟨111⟩ growth, is disturbed. After an initial stage (a few micrometers growth) a polycrystalline film with random orientation of crystal grains was formed on the top of the epitaxial film. These experiments were conducted at 900 °C and 1% of CH_4.

We continued experiments at these parameters using as substrates square plates with the (001) top surface and {110} side surfaces. At the vortex of such samples with 160 μm thick film on the top (001) surface, new crystal faces of CVD crystal appeared on the side surfaces of the substrate. This is a new (100) cube face and two triangular faces, (112) and (1$\bar{1}$2), determined by X-ray diffraction. They are shown in Fig. 8. An X-ray rotation crystal photograph was taken from the vortex area shown in the SEM image. A comparison of X-ray patterns taken with rotation parallel to the ⟨100⟩

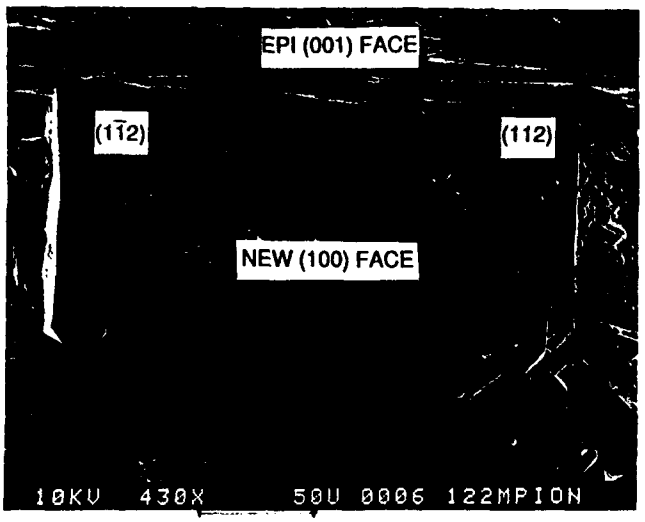

Fig. 8. New crystal faces of CVD crystal grown around the vortex of (001), (110) and (1$\bar{1}$0) surfaces of type IIa diamond crystal substrate.

direction is shown in Fig. 9. Bragg reflections from natural diamond type IIa crystal are arranged along horizontal lines.

If the reflections come from a single crystal, they are sharp and they form a regular pattern. A single crystal means that atoms lie on a line parallel to a particular crystallographic direction, and the atoms are distributed with particular periodicity. When the crystal is rotated around this line, Bragg reflections are placed on the horizontal layer lines. This is a starting point for the calculation of the repetition distance between atoms along a particular crystallographic direction ⟨*hkl*⟩ [39].

$$J = \frac{n\lambda}{\sin \mu_n} \qquad \text{where} \qquad \mathrm{tg}\mu_n = \frac{2L}{2R} \tag{1}$$

where n is the order of a horizontal line, λ is the X-ray wavelength, $2L$ is the distance between horizontal lines, $2R$ is the diameter of the cylindrical camera.

J calculated for Fig. 9(a), is 3.5 Å. This corresponds to the edge length of the unit cell of diamond. Figure 9(b) shows the diffraction pattern from the CVD film. There is a striking difference when compared with Fig. 9(a). First we see reflections (which are not sharp) located between the horizontal layer lines of cubic diamond. According to the above equation, J is larger than for cubic diamond. If we assume that reflections between the layer lines correspond to superstructure reflections, then the periodicity of cubic diamond does not appear in the CVD crystal shown in Fig. 9(b).

However, it is likely that the extra reflections appear because of some kind of twinning. To clarify the situation we developed the ⟨110⟩ growth sector with a more ordered structure. This film produced sharp reflections located on horizontal lines; this fact does not support twinning. The improvement was achieved with CVD film grown on the top and the side faces of a crystal cut along cube faces {100} Fig. 10.

The CVD film was 30 μm thick. Under crossed Polaroids the ⟨110⟩ growth sector shows birefringence indicating non-cubic structure of the crystal lattice. Attempts to generate a second harmonic were not successful. Second harmonic generation is used to establish non-center symmetry of a crystal lattice. Rotation crystal photographs were taken around the basic directions of the substrate crystal: ⟨100⟩, ⟨110⟩ and ⟨111⟩. The reflections from the ⟨110⟩ growth sectors are distinct from the (001) growth sector and from the substrate. The ⟨110⟩ growth sectors have elongated shapes (Fig. 10); corresponding X-ray reflections form elongated, but sharp spots. The superstructure reflections take positions on the horizontal layer lines between the cubic diamond layer lines. There are two such horizontal extra lines between the main horizontal lines of cubic diamond. Calculations with the help of eqn. (1) indicate that the extra reflections correspond to a superstructure with three-times larger periodicity than cubic diamond. For example, J for the ⟨100⟩ direction is 10.6 ± 0.2 Å compared with 3.5 Å calculated for cubic diamond shown in Fig. 9(a). We think, therefore, that

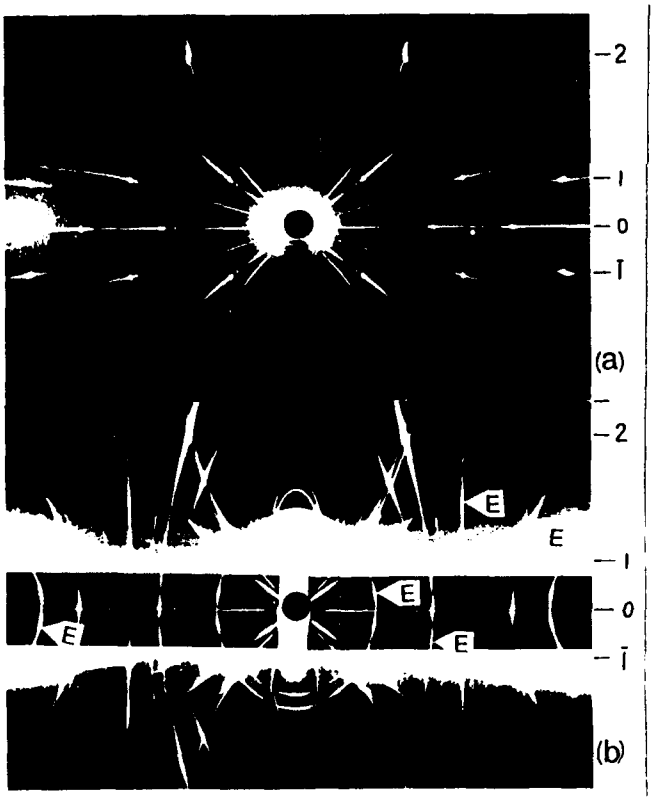

Fig. 9. Rotation crystal photograph taken with Cu radiation, filtered by Ni foil, in 57.3 mm diameter camera. Rotation direction ⟨100⟩. (a) type II diamond crystal; (b) CVD crystal, shown in Fig. 8, at the vortex of natural diamond crystal. Ni foil covers equatorial region of the film. Extra reflections are indicated by E.

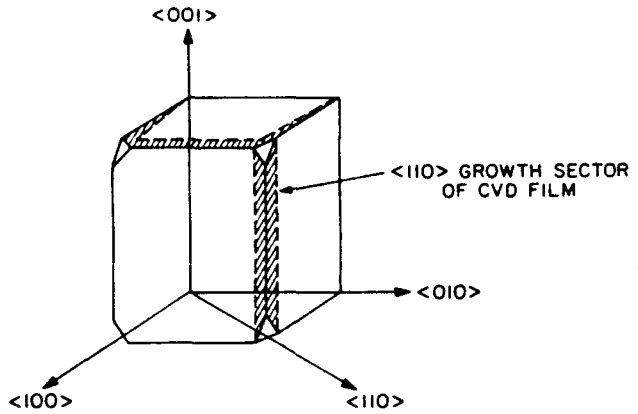

Fig. 10. Epitaxial growth on diamond crystal with cube faces. HP/HT Sumitomo Electric substrate crystal, 2 × 1.5 × 0.3 mm³.

these diffraction patterns do not correspond to twinning, because of the perfect fitting of the extra reflection to the horizontal lines.

Before a type of Bravais lattice can be assigned to the diffraction patterns we need to solve the following problem: Are we dealing with a three-dimensional superstructure or with the domains of a polytype? These domains can be arranged in a three-dimensional network, *e.g.* in eight ⟨111⟩ directions. X-ray data alone are not sufficient to solve this problem and help from TEM will be required. The spacings (d_{hkl}) of the extra reflections correspond to the cubic diamond lattice spacings within an experimental error of ±0.1 Å for a cylindrical X-ray camera (57.3 mm in diameter). Observation on deviation from the cubic symmetry, like the 2.12 Å reflection in the (111) epitaxy, will require new measurements.

Despite the fact that it is too early to make a statement about the Bravais lattice type and the lattice constants, we think, taking into account the calculations already performed, that we can anticipate a new tetrahedral network in the ⟨110⟩ growth sector. To fulfil the requirement of triple periodicity, we have proposed a polytypic structure which considers nine layers of tetrahedra. This model fulfils the requirement of threefold axis symmetry.

All published research on CVD diamond crystal structure indicate that planar defects (like twinning and stacking faults) are the defects most frequently observed by TEM and morphology studies. Our observations conducted with the help of X-ray diffuse scattering confirm the high density of planar defects in some growth sectors. As a preliminary working hypothesis we propose to consider the ordering of stacking faults or twinning, as the most likely case.

Looking at Fig. 1, we see two layers of tetrahedra for hexagonal diamond structure and three for a cubic one. We propose three unit sandwiches rotated 120° and 240°. Each sandwich unit consists of three layers of tetrahedra: two of cubic diamond sequence and one of hexagonal diamond sequence (Table 2). Because of tetrahedra shifts in the base plane of the models shown in Figs. 1(a) and 1(b), the notation (A_D,A_L) given in Table 2 does not reflect the exact position of a given tetrahedron in different consecutive sandwiches. Nevertheless three sandwiches are necessary for repetition. Such a model fulfils the requirement for triple periodicity, but does not solve the problem of three-dimensional networks.

We think that the CVD process allows tetrahedral carbon materials to be prepared with different stacking sequences. They can be a combination of cubic and hexagonal stacking. We have already made observations on how the surface reactions with active participation of other species created in the C–H gas system alter cubic diamond structure (Table 1).

Admixture of N_2 to the plasma results in enhancement of hexagonal stacking. A boron admixture has an opposite effect; it enhances cubic stacking. Epitaxy on (111) proceeds as for diamond structure which shows no luminescence feature like that shown in Fig. 5. The morphology of the (111) surface is smooth and no triangular plates appear as in Fig. 6.

Let us return to the epitaxy of cubic diamond on the (110) surface. The epitaxy was achieved at 1200 °C and 1% CH_4. This is a higher temperature range than used previously in our experiments. We were persuaded by D. V. Fedoseev to explore a high temperature regime for diamond growth [40]. Deposition took place on type IIa 2 × 2 × 0.25 mm diamond plates. Figure 11 shows a schematic diagram of CVD growth. Side (111) and (11$\bar{1}$) faces were developed. The morphology of the top (110) surface reveals very clear microfaceting with (111) and (11$\bar{1}$) planes (Fig. 12). Microfaceting is preserved after a long run (growth rate 3.5 μm h^{-1}) on the top of a prism 1.2 mm high (Fig. 12(c)).

Raman spectra taken on the top surfaces show almost

TABLE 2 Proposed stacking sequence for the ⟨110⟩ growth sector

Sandwich	First			Second			Third		
Rotation			120° ↓			240° ↓			360° ↓
Tetrahedra layer number	1	2	3	4	5	6	7	8	9
A_D diamond type						A_L	A_D	B_D	A_L
A_L lonsdaleite type	A_D	B_D	A_L	A_D	B_D	~~A_D~~ A_C	~~B_D~~	~~A_L~~	
Notation according ref. 28									
S, staggering	S	S	E	S	S	E	S	S	E
E, eclipsing									

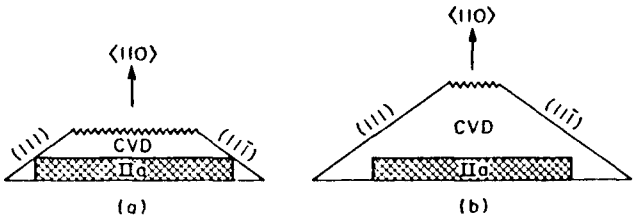

Fig. 11. Schematic representation of epitaxy in the ⟨110⟩ direction conducted at 1200 °C, 80 Torr and 1% CH_4 in H_2. CVD crystal is (a) 0.3 mm, (b) 1.2 mm thick.

no background and the FWHM of 1332 cm^{-1} peak equal 2.7 cm^{-1} (Fig. 11(a)) and 3.5 cm^{-1} (Fig. 11(b)).

Morphology of the (110) diamond surface obtained by polishing and as-grown constitute a controversial issue. Does the (110) surface corresponds to atomic plane (110) or to some kind of faceting? Our CVD growth experiments indicate (111) and (11$\bar{1}$) microfaceting.

Similar corrugation-type morphology was observed on pseudo-dodecahedral faces of natural diamond crystals which grew homoepitaxially on higher perfection octahedral cores. X-ray topography revealed branched fibrous growth along octahedral directions ⟨111⟩ + ⟨11$\bar{1}$⟩ → (110), which demonstrated that rombic dodecahedron is not a true growth form [41].

9. Conclusions

The CVD process enables crystal forms of tetrahedral carbons to be produced which are different from cubic

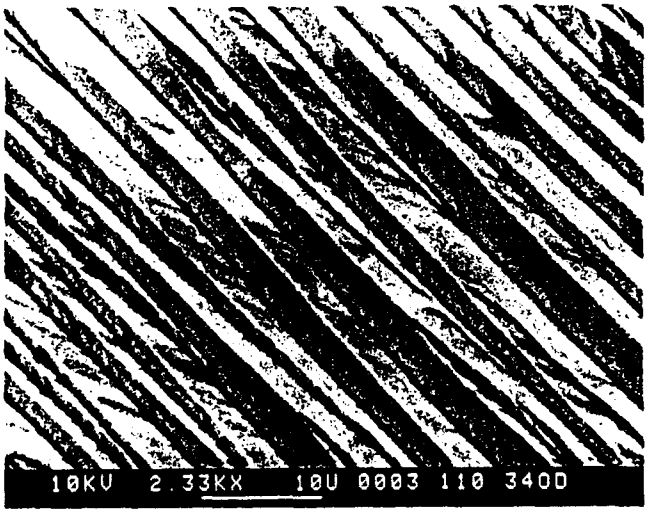

(a)

(c)

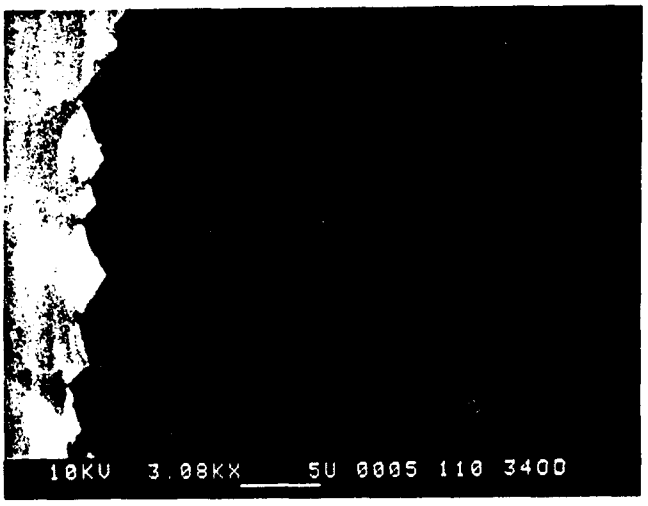

(b)

Fig. 12. Morphologies of the top surfaces shown in Fig. 11. SEM secondary electron images: (a) top view of the crystal shown in Fig. 11(a) seen over 2 × 2 mm^2 area; (b) a side view to show (111) and (11$\bar{1}$) microfaceting of the surface shown in (a); (c) top view of the crystal shown in Fig. 11(b).

diamond. We consider them as new carbon materials, however, close to diamond. When we are dealing with a new material, we need to establish its atomic structure. Assumption of cubic structure distorted by defects was not sufficient to explain X-ray data. For these reasons, we did not consider cubic structure with some defects (like stacking faults and twinning), rather, we have tried to determine individual crystal forms. These structural modifications were recognized by the diffraction patterns and the spectra which gave us a clue as to what kind of distortion of cubic structure takes place. More X-ray work is necessary to determine these structural modifications. Homoepitaxial growth revealed such anomalies as well as demonstrating the growth of nearly perfect crystals and films of cubic diamond.

Acknowledgments

00014-92-J-1421

This work was supported in part by the Office of Naval Research (with funding from the Strategic Defense Initiative Organization's Office of Innovative Technology under the contract (NO: [redacted])) and the Diamond and Related Materials Consortium at The Pennsylvania State University. This material is based in part upon work supported by the National Science Foundation under Grant No. DMR-9104072. The Government has certain rights to this material. We extend our thanks to Mark Anderson of the Jet Propultion Laboratory for his interest in imaging diamond surfaces, to William Drawl for technical assistance and for his help in Raman spectroscopy measurements, and to Ron Weimer for a critical reading of the manuscript. Thanks are extended to Professor M. Moore of the University of London for discussion on corrugated diamond surfaces.

References

1 B. V. Derjaguin and D. V. Fedoseev, The growth of diamond and graphite from diamond phase (1977), translation in *Surf. Coat. Technol., 38* (1–2) (1989) 185.
2 T. R. Antony, J. F. Banholzer, J. F. Fleischer, L. Wei, P. K. Kuo, R. L. Thomas and R. W. Pryor, *Phys. Rev. B, 42* (1990) 1104.
3 W. Banholzer, T. Antony and R. Gilmore, *Proc. 2nd Int. Conf. on New Diamond Science and Technology, Washington, DC, September, 1990*, Materials Research Society, Pittsburgh, PA, 1991 p. 857.
4 Y. Sato, Ch. Hata, T. Ando and M. Kamo, *Proc. 2nd Int. Conf. on New Diamond Science and Technology, Washington, DC, September, 1990*, Materials Research Society, Pittsburgh, PA, 1991, p. 537.
5 A. R. Badzian, T. Badzian, X. W. Wang and T. Hartnett, *Proc. 2nd Int. Conf. on New Diamond Science and Technology, Washington, DC, September, 1990*, Materials Research Society, Pittsburgh, PA, 1991, p. 549.
6 G. Janssen, W. J. P. Van Enckevort, J. J. D. Schaminee, W. Vollenberg, L. J. Gilling and M. Seal, *J. Cryst. Growth, 104* (1990) 752.
7 G. Janssen, W. Vollenberg, L. J. Gilling, W. J. P. Van Enckevort, J. J. D. Schaminee and M. Seal, *Surf. Coat. Technol., 47* (1991) 113.
8 K. A. Snail and L. M. Hanssen, *J. Cryst. Growth, 112* (1991) 651.
9 K. A. Snail, C. L. Vold, M. Marks and J. A. Freitas Jr., *Diamond Relat. Mater., 1* (1992) 180.
10 W. G. Eversole, *Synthesis of Diamond*, US Patent 3,030,188, 1962.
11 J. C. Angus, H. A. Will and W. S. Stanko, *J. Appl. Phys., 39* (1968) 2915.
12 B. V. Derjaguin, B. V. Spitsyn, A. E. Gorodetsky, A. P. Zakarow, L. L. Bouilov and A. E. Aleksenko, *J. Cryst. Growth, 31* (1975) 44.
13 B. V. Spitsyn, L. L. Bouilov and B. V. Derjaguin, *J. Cryst. Growth, 52* (1981) 219.
14 N. Fujimori, T. Imai and A. Doi, *Vacuum, 36* (1986) 99.
15 H. Nakazawa, Y. Kanazawa, M. Kamo and K. Osumi, *Thin Solid Films, 151* (1987) 199.
16 M. Kamo, H. Yurimoto and Y. Sato, *Appl. Surf. Sci., 33/34* (1988) 553.
17 M. W. Geis, Diamond, silicon carbide and related wide bandgap semiconductors, *Proc. MRS Symposium Boston, MA, November 27–December 1, 1989*, Materials Research Society, Pittsburgh, PA, Vol. 162, 1990 p. 15.
18 C. J. Chu, M. P. D'Evelyn, R. H. Hauge and J. L. Margrave, *Proc. 2nd Int. Conf. on New Diamond Science and Technology, Washington, DC, September, 1990*, Materials Research Society, Pittsburgh, PA, 1991, p. 307.
19 A. Badzian and T. Badzian, *Mater. Res. Soc. Symp. Proc., 250* (1992) 339.
20 B. E. Williams, J. F. Glass, R. F. Davis, K. Kobashi and Y. Kawate, *Mater. Res. Soc. Extended Abstracts, 15* (1988) 59.
21 W. Zhu, A. R. Badzian and R. Messier, *J. Mater. Res., 4*, (1989) 659.
22 W. Zhu, C. A. Randall, A. R. Badzian and R. Messier., *J. Vac. Sci. Technol., A7* (1989) 2315.
23 A. R. Verma and P. Krishna, *Polymorphism and Polytypism in Crystals*, Wiley, New York, 1966.
24 V. Vand, *Philos. Mag., 42* (1951) 1384.
25 S. Ergun and L. E. Alexander, *Nature, 195* (1962) 765.
26 F. P. Bundy and J. S. Kasper, *J. Chem. Phys., 46* (1967) 3437.
27 N. V. Belov, *The Structure of Ionic Crystals and Metal Phases* Izd. ANSSSR, Moscow, 1947 (in Russian).
28 W. Weltner, *J. Chem. Phys., 51* (1969) 2469.
29 K. E. Spear, A. W. Phelps and W. B. White, *J. Mater. Res., 5* (1969) 2469.
30 M. Frenklach, R. Kematick, D. Huang, W. Howard, K. E. Spear, A. W. Phelps and R. Koba, *J. Appl. Phys., 66* (1989) 395.
31 Cover page, *Science, 250*, 21 December (1990) (60 μm thick CVD film).
32 B. G. Yacobi, I. Lebens, K. I. Vahala, A. R. Badzian and T. Badzian, *Proc. 3rd Int. Conf. on New Diamond Science and Technology, Heidelberg, Germany, August 31–September 4, 1992, Diamond Relat. Mater., 2* (1993) XXX.
33 D. J. Chadi, *Phys. Rev. Lett., 59* (1987) 1691.
34 T. Tsuno, T. Imai, Y. Nishibayashi, K. Hamada and N. Fujimori, *Jpn. J. Appl. Phys., 30* (1991) 1063.
35 A. Badzian, M. Wisniewska, B. Widaj, B. Krukowska-Fulde and T. Niemyski, *J. Cryst. Growth, 5* (1969) 222.
36 B. B. Pate, *Surf. Sci., 165* (1986) 83.
37 T. Evans and D. H. Sauter, *Philos. Mag., 6* (1961) 429.
38 A. Badzian, T. Badzian and X. H. Wang, *Carbon, 28* (1990) 804.
39 B. E. Warren, *X-ray Diffraction*, Addison-Wesley, Reading, MA., 1969, p. 86.
40 I. G. Varshavskaja and A. V. Lavrientiev, *Arch. Nauk. Material., 7* (1986) 83.
41 W. G. Machado, M. Moore and G. S. Woods, *J. Cryst. Growth, 71* (1985) 718.